DISCLAIMER

This report was prepared as an account of work sponsored by an agency of the United States Government. Neither the United States Government nor any agency thereof, nor any of their employees, makes any warranty, express or implied, or assumes any legal liability or responsibility for the accuracy, completeness, or usefulness of any information, apparatus, product, or process disclosed, or represents that its use would not infringe privately owned rights. Reference herein to any specific commercial product, process, or service by trade name, trademark, manufacturer, or otherwise does not necessarily constitute or imply its endorsement, recommendation, or favoring by the United States Government or any agency thereof. The views and opinions of authors expressed herein do not necessarily state or reflect those of the United States Government or any agency thereof. Reference herein to any social initiative (including but not limited to Diversity, Equity, and Inclusion (DEI); Community Benefits Plans (CBP); Justice 40; etc.) is made by the Author independent of any current requirement by the United States Government and does not constitute or imply endorsement, recommendation, or support by the United States Government or any agency thereof.

LA-UR-25-25192

Approved for public release; distribution is unlimited.

Title:	LANL ACRSP Parameter Recommendations for CRA-2026 Performance Assessment
Author(s):	Swanson, Juliet S. Kaplan, Ugras Kutahyali Aslani, Ceren
Intended for:	Report
Issued:	2025-06-02

LOS ALAMOS NATIONAL LABORATORY
CARLSBAD OPERATIONS

LCO-ACP-41, Revision 1

LANL ACRSP Parameter Recommendations for CRA-2026 Performance Assessment

Effective Date: 05/28/2025

Originators:

Ugras Kaplan — Digitally signed by Ugras Kaplan Date: 2025.05.27 09:17:00 -06'00'

Ugras Kaplan, LANL-CO ACRSP — Date

JULIET SWANSON (Affiliate) — Digitally signed by JULIET SWANSON (Affiliate) Date: 2025.05.27 08:56:04 -06'00'

Julie Swanson, LANL-CO ACRSP — Date

Ceren Kutahyali Aslani — Digitally signed by Ceren Kutahyali Aslani Date: 2025.05.27 08:57:42 -06'00'

Ceren Kutahyali Aslani, LANL-CO ACRSP — Date

Reviewed By:

JEAN FRANCOIS LUCCHINI (Affiliate) — Digitally signed by JEAN FRANCOIS LUCCHINI (Affiliate) Date: 2025.05.27 10:17:14 -06'00'

Jean-François Lucchini, LANL-CO ACRSP — Date

Approved by:

JONATHAN ICENHOWER (Affiliate) — Digitally signed by JONATHAN ICENHOWER (Affiliate) Date: 2025.05.28 09:08:36 -06'00'

Jonathan Icenhower, LANL-CO ACRSP Team Leader — Date

PRISCILLA YANEZ (Affiliate) — Digitally signed by PRISCILLA YANEZ (Affiliate) Date: 2025.05.28 09:20:40 -06'00'

Priscilla Yanez, LANL-CO Quality Assurance Manager — Date

DOUGLAS WEAVER (Affiliate) — Digitally signed by DOUGLAS WEAVER (Affiliate) Date: 2025.05.28 09:45:50 -06'00'

Douglas Weaver, LANL-CO Division Leader — Date

History of Revisions

Revision Number	Effective Date	Pages Affected	Description of Revision
0	03/26/2025	All	Original Release
1	05/28/2025	1, 2, 7-10, 12, 17, 19	Revised to address comments from DOE.

Executive Summary

This report provides recommendations made by the Los Alamos National Laboratory—Carlsbad Operations (LANL-CO) Actinide Chemistry & Repository Science Program (ACRSP) for the following parameters used in the 2026 Compliance Recertification Application (CRA) Performance Assessment (PA) calculations: OXCUTOFF, CONCMIN, CONCINT, CAPMIC, PROPMIC, and SOLMOD (SOLCOH and SOLSOH). A summary of the values recommended for the WIPP parameters are included in the Tables below. The shaded cells indicate a change from the CRA-2019 recommended values. A short summary of the basis and justification for each parameter and recommendation is given in this document.

Table 1. Element-based parameter recommendations for CRA-2026

Parameter Values Recommended for CRA-2026 (Part I, Element-Based)				
Actinide	OXCUTOFF	SOLMOD (M)	Colloids	
			Mineral	Intrinsic
			CONCMIN (M)	CONCINT (M)
Th	1	N/A	2.60×10^{-8}	4.80×10^{-7}
U	0.5	3.00×10^{-6}	2.60×10^{-8}	1.40×10^{-6}
Np	0.5	N/A	2.60×10^{-8}	4.30×10^{-8}
Pu	0.25	N/A	2.60×10^{-8}	4.30×10^{-8}
Am	1	N/A	2.60×10^{-8}	6.70×10^{-7}

Table 2. Oxidation state-based parameter values for CRA-2026

Parameter Values Recommended for CRA-2026 (Part II, Oxidation State-Based)		
Actinide and Oxidation State	Microbial Colloids	
	CAPMIC (M)	PROPMIC
Th(IV)	6.95×10^{-4}	3.10×10^{0}
U(IV)	9.65×10^{-6}	2.10×10^{-3}
U(VI)		
Np(IV)	1.52×10^{-7}	1.20×10^{1}
Np(V)		
Pu(III)	4.97×10^{-7}	2.92×10^{0}
Pu(IV)	4.07×10^{-9}	3.00×10^{-1}
Am(III)	4.97×10^{-7}	2.92×10^{0}

Table of Contents

Acronyms, Abbreviations, Formulas

ACRSP	Actinide Chemistry and Repository Science Program (LANL-CO)
Am	Americium
An	Actinide
CAPMIC	Colloid parameter for the maximum concentration of actinide associated with mobile microbes
CBFO	Carlsbad Field Office (DOE)
CCA	Compliance Certification Application
Ci	Curie
Cm	Curium
CONCINT	Parameter for the concentration of actinide associated with mobile intrinsic actinide colloids
CONCMIN	Parameter for the concentration of actinide associated with mobile mineral fragment colloids
CRA	Compliance Recertification Application
d	Day
DOE	Department of Energy
EDTA	Ethylenediaminetetraacetic acid
E_h	Redox potential
EPA	Environment Protection Agency
ERDA-6	Energy Research and Development Administration Well-6 (WIPP brine)
EXAFS	Extended X-ray Absorption Fine Structure
Fe	Iron
Fe^0	Metallic iron
Fe_3O_4	Magnetite, an iron(II,III) -oxide mineral with the chemical formula $Fe^{2+}Fe_2^{3+}O_4^{2-}$
$Fe(OH)_2(cr)$	Ferrous hydroxide, crystal
GWB	Generic Weep Brine (WIPP high Mg brine)
g	Gram
L	Liter
LANL-CO	Los Alamos National Laboratory-Carlsbad Operations
M	Moles per liter
mg	Milligram
MgO	Magnesium oxide – engineered barrier for the WIPP
ml	milliliter
mM	Millimoles per liter

Acronyms, Abbreviations, Formulas (cont.)

mV	Millivolt
NaCl	Sodium chloride
Nd	Neodymium
nm	Nanometer
Np	Neptunium
OXCUTOFF	PA parameter indicating the fractional value for the lower oxidation state of an element
OXSTAT	PA indicator variable for elemental oxidation states
PA	Performance Assessment
pC_{H+}	Negative logarithm of the hydrogen ion concentration (pH corrected for high ionic strength)
pH	Negative logarithm of hydrogen ion activity
PROPMIC	Proportionality constant for the concentration of actinides associated with mobile microbes
Pu	Plutonium
SNL	Sandia National Laboratories
SOLMOD	PA solubility parameter
SOTERM	Actinide Source Term (Appendix for the WIPP CRA)
Th	Thorium
TRU	Transuranic
U	Uranium
WIPP	Waste Isolation Pilot Plant
XANES	X-ray Absorption Near-Edge Spectroscopy
XAS	X-ray Absorption Spectroscopy

1.0 Introduction

The Waste Isolation Pilot Plant (WIPP) transuranic (TRU) waste repository continues to be the cornerstone of the United States nuclear waste management effort. As a condition of operation, the Environmental Protection Agency (EPA) is to recertify the WIPP every five years. The five-year recertification period was changed from application-to-application to completeness determination-to-application (EPA, 2023). The last Compliance Recertification Application (CRA) was submitted to the EPA in March 2019 and was determined complete in November, 2021 (DOE, 2019).

The Los Alamos National Laboratory—Carlsbad Operations (LANL-CO) Actinide Chemistry and Repository Science Program (ACRSP) team has routinely provided recommendations for WIPP Performance Assessment (PA) parameters regarding actinide solubility, oxidation state, and colloids, at the request of Sandia National Laboratories (SNL) PA group (Reed et al., 2019; Lucchini and Swanson, 2023; King, 2025). This report contains updated recommendations from LANL-CO ACRSP for parameter values to be used in the CRA-2026 PA.

A review of parameter definitions, the recommended parameter values, and the basis and justification for these recommendations are presented in the following sections.

2.0 Actinide Oxidation State Distribution

The WIPP project has had the same conceptual model for the oxidation state distribution of TRU actinides since the original Compliance Certification Application (CCA) (DOE, 1996). The actinide model reflects the expected post-closure conditions in the repository: anoxic with excess zero-valent iron and potential saturation of the repository horizon with magnesium oxide (MgO, engineered barrier)-reacted high ionic strength brine. Taking into account these conditions, the oxidation state model covers a range in E_h that brackets the expected conditions and implements a set of actinide oxidation states for the least and most reducing conditions. This is discussed in detail in the CRA-2019 documentation (DOE Appendix SOTERM-2019; DOE Appendix PA-2019).

Since the CCA, the WIPP actinide oxidation state distribution model has been based on two sets of oxidation states that govern actinide solubility. The first set, “low”, includes Pu(III), Np(IV), and U(IV). The second set, “high”, includes Pu(IV), Np(V), and U(VI). The redox-invariant thorium, americium, and curium are not included in these sets. In PA, the release calculations use the OXCUTOFF and OXSTAT parameters to indicate the actinide oxidation state distribution. OXCUTOFF designates the fractional value for the lower oxidation state of the actinide and has a fixed value between 0 and 1. OXSTAT is a sampled value between 0 and 1 that determines the oxidation state in specific realizations. When the value of OXSTAT is sampled below OXCUTOFF, the lower oxidation state is dominant and controls the solubility of the element; if the OXSTAT value is above OXCUTOFF, the higher oxidation state prevails and controls solubility (DOE Appendix PA-2019).

Since the initial CCA, the actinide oxidation state distributions have been parameterized in PA as follows:

All PA vectors (100 % probability)	Am(III), Cm(III) and Th(IV)
Least reduced PA vector (50 % probability)	U(VI), Np(V) and Pu(IV)
Most reduced PA vector (50 % probability)	U(IV), Np(IV) and Pu(III)

The oxidation state distribution of the actinides in the WIPP PA continues to be a point of discussion with the EPA, particularly in the case of plutonium. A recent literature review was conducted by Schramke et al. "to evaluate the effects of WIPP chemical and physical processes on dissolved (not colloidal) plutonium oxidation states that included reactions with reducing agents such as iron solids and aqueous species and radiolysis of solids and aqueous species" (Schramke et al., 2020). The main conclusion of the study was that "extremely reducing conditions, including the presence of metallic iron, $Fe(OH)_2$(cr) and/or magnetite will lead to plutonium solubility control by Pu(III) solid." This conclusion directly challenges the WIPP 50:50 oxidation state distribution for plutonium. Most recently, the EPA has indicated that DOE should assume that the Pu oxidation state is 100 % Pu(III) (EPA, 2022).

Basis and Justification for the Parameter Recommendation for Pu

LANL-CO ACRSP is concluding long-term Pu solubility experiments that provide the first experimental data obtained under WIPP-relevant conditions to support a realistic oxidation state ratio for Pu in the WIPP PA model (Beam, 2023; Kaplan, 2024a). In these experiments, the oxidation state distribution and solubility of plutonium were comprehensively examined both in the presence and absence of metallic iron and magnetite, as well as in the presence and absence of four organic ligands relevant to the WIPP—oxalate, acetate, citrate, and EDTA—in an alkaline WIPP brine solution within a pC_{H+} range of 8-10.

Waste containers, particularly steel drums, represent a significant source of iron in nuclear waste repositories. The corrosion of these generates a reducing environment that can influence the solubility and binding behavior of certain actinides, specifically by reducing their oxidation states. In this experimental study, two distinct corrosion products were selected to simulate the range of redox potentials (E_h) that may develop in the WIPP following repository closure. This approach aimed to enhance the accuracy of modeling future repository conditions.

The selection of magnetite, to represent the upper E_h boundary, is justified by several critical factors (Asami and Kikucki, 2003; Cook, 2005; King, 2008). Proper assessment of corrosion product formation requires an accurate understanding of the evolving chemical conditions within a nuclear waste repository. Before the onset of anoxic conditions, the repository environment will remain oxic for a certain period of time. During this initial phase, the available oxygen will gradually be depleted, resulting in the coating of containers with a corrosion layer rich in Fe(III). As repository conditions become more anoxic, Fe(III)-containing phases within the corrosion film will become thermodynamically unstable and will undergo progressive reduction to Fe(II) species. Throughout the anoxic phase, this reduction process facilitates the formation of magnetite, a mixed-valence iron oxide ($Fe^{2+}Fe_2^{3+}O_4^{2-}$) that is thermodynamically stable under

anoxic conditions. Empirical observations support this expectation, as magnetite has been identified as a key corrosion product in steel bridges and other iron-based structures exposed to marine environments (Asami and Kikucki, 2003; Cook, 2005).

An additional argument supporting the persistence of Fe(III) in the WIPP system arises from the radiolysis effects induced by Pu-239. Radiolytic processes have been shown to generate localized oxic conditions, an effect extensively discussed in both experimental and theoretical studies. Investigations in saline solutions have demonstrated that alpha radiation significantly influences the redox chemistry and complexation behavior of actinides. These effects are dependent on chloride concentration and overall activity levels. In simplified brine systems (e.g., NaCl solutions), radiolysis has been observed to promote oxidation and elevate E_h values (Büppelmann et al., 1986, 1988; Kim et al., 1987; Pashalidis et al., 1993; Garnov et al., 1998).

Based on the factors outlined above, we anticipate that Fe(III) will contribute to the composition of corrosion products within WIPP. In the LANL-ACRSP study, magnetite—an Fe(II)/Fe(III)-containing, thermodynamically stable corrosion product—was selected to reflect the expected post-closure redox conditions of the WIPP nuclear waste repository.

One of the key aspects of this study is the analysis of the Pu oxidation state and speciation, both on the surface area of the corrosion products and in the precipitated solid phase. This dual sampling approach has not been previously reported in the literature. Figure 1 illustrates the preparation of the samples for the analysis of the oxidation state of Pu. Furthermore, the analysis of the Pu oxidation state on the surface of the iron mineral in the ongoing undersaturated solubility experiments (1200 days) is more relevant to the performance assessment of nuclear waste disposal systems than short-term batch experiments (such as plutonium-iron phase experiments like those conducted by Kirsch et al., 2011, Dumas et al., 2019). An additional advantage of the 800-day duration is a better consideration of radiolysis effects by Pu-239, which is critical for accurately assessing long-term behavior.

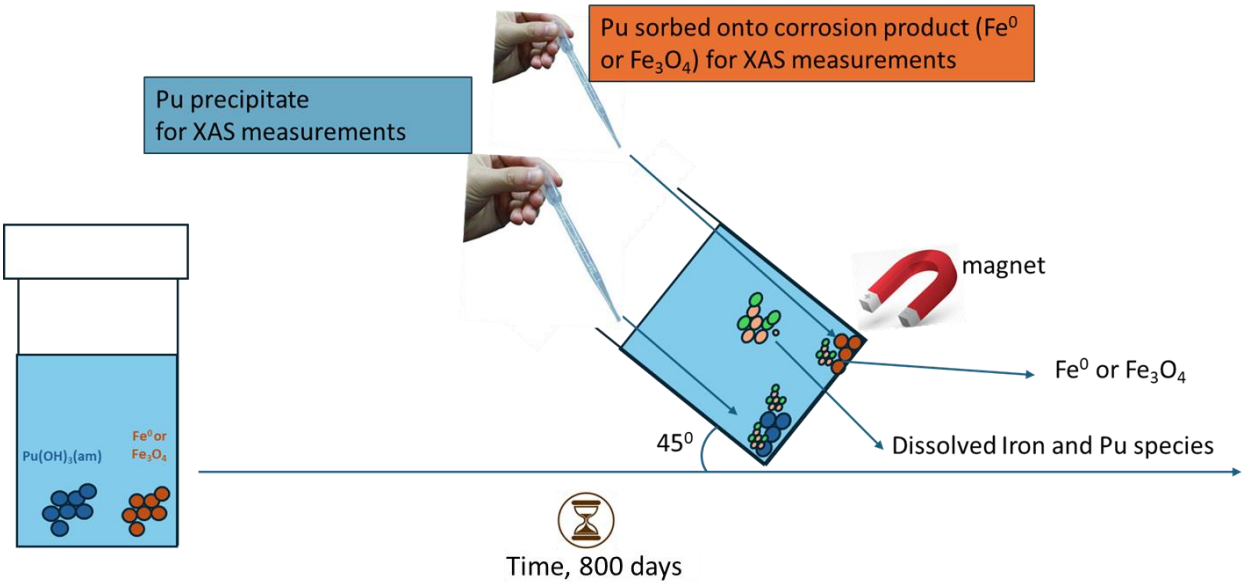

Figure 1. Preparation of samples for XAS analysis of Pu oxidation state (from Kaplan, 2024a).

Samples were prepared for oxidation state analysis by X-ray Absorption Spectroscopy (XAS), as shown in Figure 1, without disturbing their built-in conditions, and were measured under anoxic conditions using the non-destructive XAS method at the Stanford Synchrotron Radiation Lightsource. In addition, plutonium speciation at the molecular level was determined by Extended X-ray Absorption Fine Structure (EXAFS) analysis.

Figure 2 shows the oxidation states distribution calculated using linear combination fit analysis in both the precipitated solid phase and on the surface of iron corrosion products, in the presence and absence of organics. EXAFS analysis showed that while Pu did not form complexes with any of the brine component salts, it did complex with the iron corrosion products.

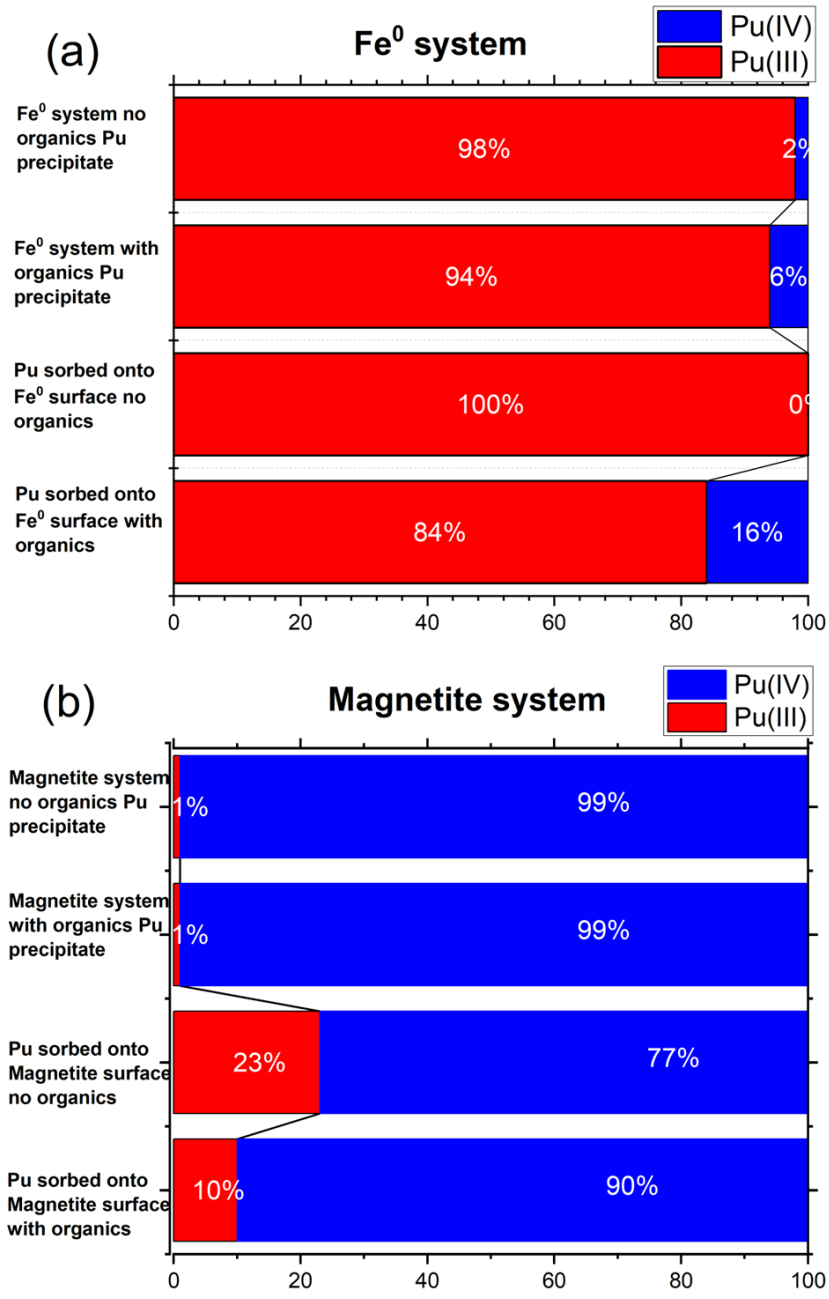

Figure 2. The oxidation state distribution of Pu in both precipitate solid phases and on the surface of iron corrosion products in the presence and absence of organics.

X-ray Absorption Near-Edge Spectroscopy (XANES) analysis showed that Pu oxidation state was different on the metal surface and in the precipitated solid. Pu(III) was the dominant oxidation state in the metallic iron (Fe^0) systems in the presence and absence of organics and in both the precipitated solid Pu phase and the Pu phase on the metallic iron surface (Figure 2a). In contrast, Pu(IV) was the dominant oxidation state in the magnetite systems in the presence and

absence of organics and in both the precipitated phase and the sorbed phase (Figure 2b). Additionally, organics stabilized Pu(IV) in the magnetite systems.

The most important reason for these findings is the redox potential. In WIPP brines containing metallic iron, the E_h values measured between -300 and -437 mV, reflecting a strongly reducing environment that stabilized Pu(III). In contrast, the E_h values in the magnetite system ranged between +30 and +309 mV, representing a more oxidizing environment that favored the predominance of Pu(IV). This highlights the importance of the iron corrosion product selection and shows that the choice of corrosion products in these experiments successfully bounds the possible redox conditions at the WIPP.

The presence or absence of organics in the system did not affect the oxidation state of Pu as strongly as the corrosion products. The Pu(III)/Pu(IV) ratios between samples with and without organics were within 10-15 %. However, previous studies and current preliminary work have demonstrated that alpha radiation from Pu-239 will lead to the degradation of organic compounds (Toste, 1992; Toste et al., 1994; Favela Morales and Lucchini, 2023). Therefore, the effect of organics will become even less significant over time.

The EPA has questioned the representativeness of the LANL-ACRSP experiments to WIPP conditions, specifically the Pu-to-iron ratio and the choice of magnetite, as opposed to a more reduced iron phase. The data presented here clearly show that the choice of iron corrosion product is extremely important. The use of magnetite is justified by its acceptance in the literature as the most likely solid phase produced from the anoxic corrosion of steel and iron in both field and experimental observations (Asami and Kikucki, 2003; Cook, 2005; Hara et al., 2007; Krolikowska et al., 2021). In addition, it is the most thermodynamically stable phase found in most assessments of redox conditions in underground repositories for radioactive waste (Duro et al., 2014; Saheb et al., 2010).

In the LANL-ACRSP experiments, 2 mg of Pu were used per 100 mg of iron corrosion product. The actual ratio at closure is projected as 5.13×10^{-4} g Pu/g Fe or 6.17×10^{-5} Curie (Ci) Pu/g Fe, based on the iron-based metal/alloys and steel inventories (Van Soest, 2022, Tables 5-3 through 5-5). Given the well-documented affinity of Pu for iron minerals, if a higher mass of iron had been used in this study (i.e., the actual Pu/Fe ratio), the Pu concentration would have fallen below the detection limit, making it impossible to measure oxidation states with XANES and speciation with EXAFS. After 10,000 years, the ratio is even lower (3.68×10^{-4} g/g or 2.51×10^{-5} Ci/g). The 2/100 ratio was chosen in order to obtain solubility data and to be able to analyze samples for oxidation state distributions.

To best adapt the findings from these experiments to long-term WIPP conditions, we elected to neglect the effect of organic compounds, since they are expected to degrade over time, due to radiolytic, if not microbial, degradation. In addition, the oxidation state evaluation should focus on the magnetite surface, rather than the bulk precipitates, given that Pu interactions with solid phases primarily occur through surface adsorption. This provides the rationale for using the magnetite-no organic test system as the basis for the OXCUTOFF parameter. While XAS research does not typically involve multiple replicate samples so much as multiple scans (e.g., 10

in this case), the XANES analyses presented in Kaplan (2024a, 2024b) were multi-modal, comparing absorption edge, white line, and linear combination fit analysis (an advanced form of data interpretation), thus strengthening the robustness of the data.

Considering these recent ACRSP findings and studies in the literature, a change in Pu oxidation state distribution is currently recommended. It is proposed that 75 % of the PA vectors contain Pu(IV) and 25 % contain Pu(III) (Table 3). This reflects the ratio obtained on the magnetite surface without organics. No changes are proposed for the other actinides in the WIPP actinide oxidation state model.

Table 3. CRA-2026 recommended values for the OXCUTOFF parameter for Pu, Np and U

Parameter Values for OXCUTOFF Recommended for CRA-2026	
Pu	0.25
Np	0.50
U	0.50

3.0 Actinide Solubility Parameters—An(VI)

The WIPP Actinide Source Term Program did not develop a model for the solubility of actinides in the VI oxidation state. In the absence of WIPP-specific data, the EPA specified that 1×10^{-3} M be used as the An(VI) solubility value for the Performance Assessment Baseline Calculation, and this value has been used in all subsequent WIPP compliance calculations (EPA, 2005).

Basis and Justification for the Recommended Values for U(VI) Solubility

A detailed report and data summary with recommendations for An(VI) solubility values was issued by LANL-ACRSP, describing experiments on U(VI) solubility in WIPP-relevant brines as a function of pC_{H+} and ionic strength, both in the presence and absence of carbonate. The uranium (VI) solubilities in these experiments were ~10^{-6} M in GWB at $pC_{H+} \geq 7$ and between 10^{-8} and 10^{-7} M in ERDA-6 at $pC_{H+} \geq 8$. At the expected pC_{H}^{+} in the WIPP (~ 9.5), uranium solubility approached between 10^{-7} and 10^{-6} M. In experiments investigating the effect of carbonate on uranium solubility in WIPP brines, the highest uranium concentration was measured at ~10^{-4} M. This was in experiments with the highest tested carbonate concentration (2×10^{-3} M), which is ~10 times higher than the carbonate concentration predicted by WIPP PA (Lucchini et al., 2010, 2013; Appendix GEOCHEM-2019).

Recent U(VI) solubility experiments have been performed by LANL-ACRSP in anoxic 90%-capacity WIPP brine at pC_{H+} 9, with different borate concentrations, and in the presence of relevant organics (EDTA, oxalate, citrate, and acetate), using an under-saturation approach, to determine the effects of organics and borate on uranium solubility (Kutahyali Aslani, 2024). The results show that the solubility of uranium was higher when all WIPP-relevant organics were present, and that this increased solubility was predominantly due to citrate complexation (Figure

3). Although increasing concentrations of borate slightly increased uranium solubility, at the WIPP-relevant borate concentration, the solubility was only ~10^{-6} M (Figure 4).

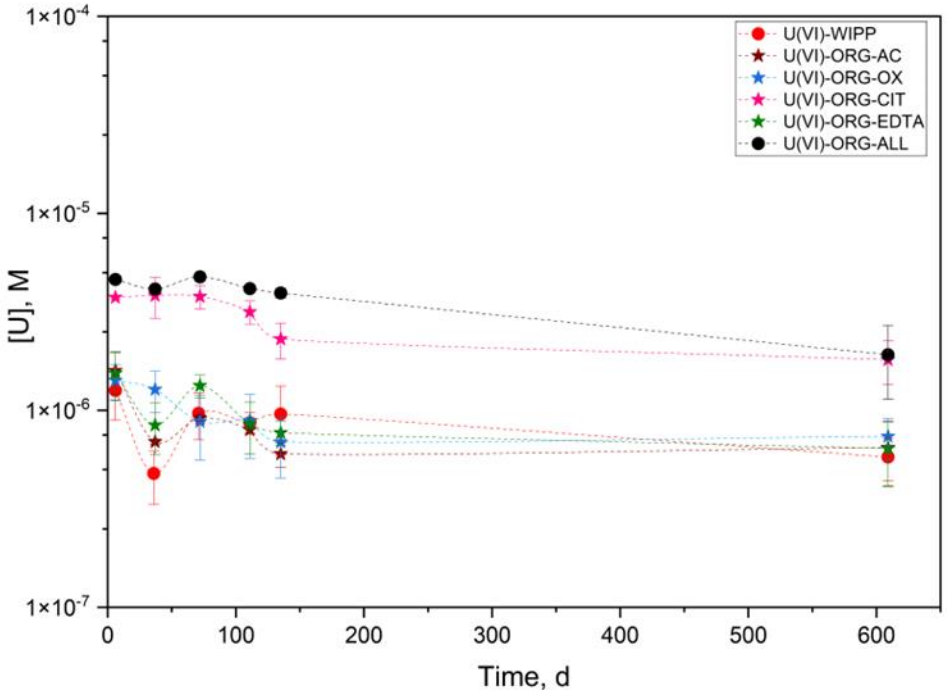

Figure 3. Effect of organics on uranium solubility as a function of time in pC_{H+} 9 brine (AC = acetate; OX = oxalate; CIT = citrate). From Kutahyali Aslani, 2024.

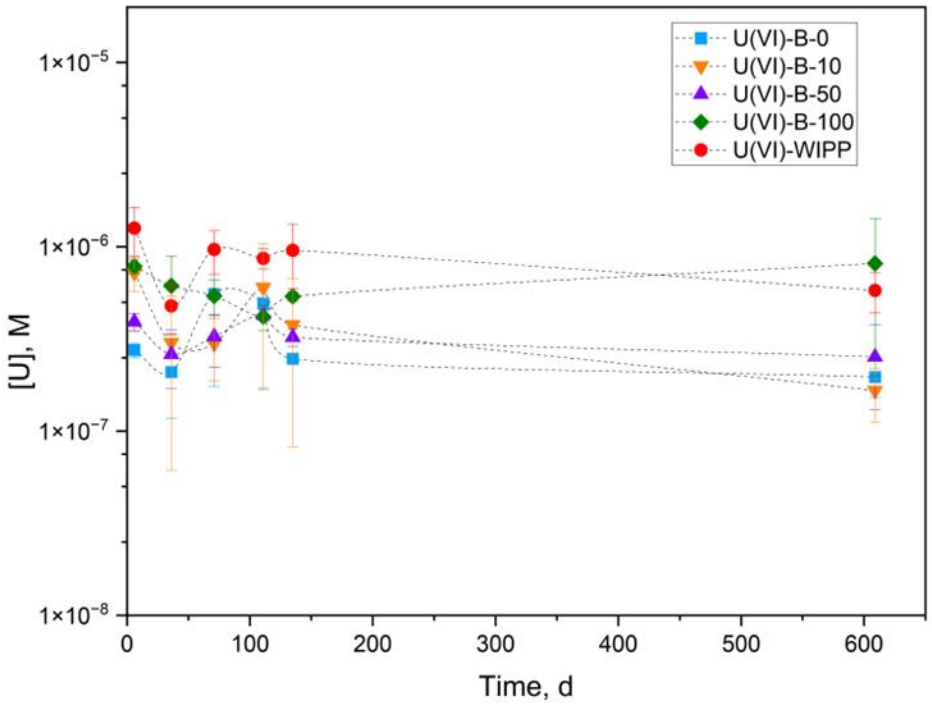

Figure 4. Effect of borate on uranium solubility as a function of time in pC_{H+} 9 brine (B = borate, concentrations in mM; WIPP concentration set to 140 mM). From Kutahyali Aslani, 2024.

The results of this work, in conjunction with those of Lucchini et al. (2010, 2013) support the introduction of a new solubility parameter for An(VI). The EPA specification for uranium solubility (1×10^{-3} M) was proposed based on the potential influence of carbonate. Although Kutahyali Aslani (2024) did not use carbonate in her experiments, the concentrations of organic ligands used were approximately 40 times higher than the expected carbonate concentration, and uranium solubility was less than 10^{-5} M (Figure 3). Lucchini et al. (2007, 2013) used two carbonate concentrations, the lowest of which (2.0×10^{-4} M) approximates the calculated mean value for total inorganic carbon in WIPP brines (2.35×10^{-4} M; Appendix GEOCHEM-2019). At this tested concentration, uranium solubility was ~1.0×10^{-6} M. This value, derived from an oversaturation approach, is similar to the value from the organic work, which used an undersaturation approach ($1.77 \pm 0.77 \times 10^{-6}$ M). We have taken the values from both works (average $1.48 \pm 1.12 \times 10^{-6}$ M), applied a ~40% margin of error to achieve ~ 95% confidence, and rounded up to result in 3×10^{-6} M for the recommended SOLMOD6 parameter (Table 4).

Table 4. Parameter values for An(VI) solubilities recommended for CRA-2026.

Material	Property	Value
SOLMOD6	SOLCOH	3.00×10^{-6} M
SOLMOD6	SOLSOH	3.00×10^{-6} M

4.0 Colloid Enhancement Parameters

The following sub-sections address the recommended parameter values for mineral, intrinsic, and microbial colloids.

4.1 Mineral Colloids

The mineral fragment colloidal contribution to the WIPP mobile actinide source term is defined by the CONCMIN parameter:

CONCMIN: Concentration of actinide associated with mobile mineral fragment colloids (moles of mineral-bound actinide per liter). This is implemented in PA as an element-specific parameter.

As of CRA-2014, this is defined operationally as actinide colloidal species > 10 nm when mineral colloids are known to be present in WIPP brine (Reed et al., 2013).

Since the CRA-2019, only one experimental study in WIPP-relevant systems has been reported regarding mineral colloids of actinides. In response to the EPA issues list, the LANL ACRSP team investigated the effect of dissolved silica on the solubility of An(III) and An(IV) solids, as well as the possibility of actinide-silica colloid formation, in 5 M NaCl solutions (Beam, 2022; EPA, 2022). At pH values relevant to WIPP, no significant colloid fraction was observed, as measured by sequential filtration. Additionally, no increase in solubility was observed in the presence of sodium metasilicate. This suggests that actinide-silica colloids will not form in a direct brine release scenario into the repository.

Therefore, there are no changes recommended for the CONCMIN parameter values used by WIPP PA. The recommended values for the CONCMIN parameter for all actinides and oxidation states are identical to those used in the CRA-2019. They are summarized in Table 5.

Table 5. Values for the actinides recommended for the CONCMIN parameter in CRA-2026.

Parameter values for CONCMIN recommended for CRA-2026	
Actinide	CONCMIN (M)
Th	2.60×10^{-8}
U	2.60×10^{-8}
Np	2.60×10^{-8}

Parameter values for CONCMIN recommended for CRA-2026	
Actinide	CONCMIN (M)
Pu	2.60×10^{-8}
Am	2.60×10^{-8}

4.2 Intrinsic Colloids

The intrinsic colloidal contribution to the WIPP mobile actinide source term is defined by the CONCINT parameter:

CONCINT: Concentration of actinide associated with mobile intrinsic actinide colloids (moles/L). This is implemented in PA as an element-specific parameter.

Although intrinsic colloids are more dependent on oxidation state than element, they are implemented in PA as element-specific values (Reed et al., 2019). As of CRA-2014, these were operationally defined as between 2.5 and 10 nm in size, based on filtration. For CRA-2019, the data in (Reed et al., 2013; Section 4.2 and 4.4) were re-examined over a broader pH range, and updated values for the CONCINT parameter were recommended and used in the WIPP PA.

There have been no new WIPP-relevant data on intrinsic colloids since the CRA-2019. However, the EPA proposed the following changes to the CONCINT parameter for Am and Th (EPA, 2022):

- Increase the Am intrinsic colloid concentration from 9.5×10^{-9} M, used in the CRA-2019 PA calculations (Reed et al., 2019), to 6.7×10^{-7} M (EPA, 2022; Section 8.1.4), which is the upper bound concentration for the long-term Nd(III) solubility experiments carried out by Borkowski et al. (2010) and revisited by Reed et al. (2013).
- Increase the Th intrinsic colloid concentration from 4.3×10^{-8} M (Reed et al., 2019) to a value of 4.8×10^{-7} M (EPA, 2022 Section 8.1.5), which appears to be more consistent with the Th(IV) experimental data considered in the WIPP PA (Altmaier et al., 2004; Borkowski, 2012).

Although the two changes proposed by EPA are an increase of about one to two orders of magnitude, we do not have data from new experiments that refute this proposal. Therefore, the two changes proposed by the EPA are accepted. The values for the CONCINT parameter recommended for CRA-2026 are included in Table 6.

Table 6. Values for the actinides recommended for the CONCINT parameter in CRA-2026.

Parameter values for CONCINT recommended for CRA-2026	
Actinides	CONCINT (M)
Th	4.80×10^{-7}
U	1.40×10^{-6}
Np	4.30×10^{-8}
Pu	4.30×10^{-8}
Am	6.70×10^{-7}

4.3 Microbial Colloids

Two parameters are used in PA to represent the microbial colloid contribution to the mobile actinide concentration—PROPMIC and CAPMIC:

PROPMIC: proportionality constant for the concentration of actinides associated with mobile microbes (moles of microbe-bound actinide/moles of dissolved actinide).

CAPMIC: maximum concentration of actinide associated with mobile microbes (moles of microbe-bound actinide/L).

From the CCA through CRA-2009, these values were provided based on element. For CRA-2014, two sets of values were presented: element-specific and oxidation state-specific. As there are no new data for oxidation states other than An(III), the recommended parameters for both oxidation states of uranium and neptunium will be the same.

As a result of continued discussion with the EPA, the DOE has reassessed the 2014 and 2019 parameter values. The EPA requested that the original CCA values be used “until DOE provides more experimental data to adequately justify an update”, but the EPA also suggested new values (EPA, 2022). The DOE has agreed to return to the CCA PROPMIC values, with the exception of any element in the +3 state, since there are now sufficient WIPP-relevant data to support its case.

The EPA also recommended that DOE use CAPMIC values generated from the original Papenguth (1996) data but recalculated to conform with the biomass-based approach (Peake, 2020). However, the CCA experiments were toxicity-based and were not designed to target a high, fixed biomass concentration (10^9 cells/ml). To be self-consistent with methodology, DOE has chosen to use the data from the CCA filtration studies as presented in Francis et al. (1998), as this approach adheres more closely to the definition of CAPMIC. Even so, the biomass concentrations in those experiments were often very low, such that using the high, fixed multiplier unreasonably overestimates the CAPMIC values to concentrations that exceed inventory (e.g., Th; Table 7). In those cases, the actual biomass concentration was used.

Table 7. Comparison between CAPMIC values calculated from CCA data with and without the high biomass concentration multiplier.

Element	CAPMIC values based on actual biomass	CAPMIC values based on fixed multiplier
Pu	1.22×10^{-9}	4.07×10^{-9}
Th	6.95×10^{-4}	1.88×10^{0}
Np	2.33×10^{-6}	1.01×10^{-3} (bac), 1.52×10^{-7} (arch)
U	2.22×10^{-6}	9.65×10^{-6}

Basis, Justification, and Calculations for Recommendations for An(IV-VI)

As mentioned above, the DOE has agreed to return to the CCA PROPMIC values for these oxidation states. The DOE has also recalculated CAPMIC values to adhere to the biomass-based approach, per the EPA's request, with the exceptions noted above. The data are taken from Francis et al., 1998 (as reported in Papenguth, 1996). Archaeal data were used to calculate all except Th, for which there were only bacterial data available.

- Pu(IV-VI): [(1.22×10^{-9} M associated with cells)/(3.0×10^{11} cells/L)]*10^{12} cells/L = 4.07×10^{-9} M
- Th(IV): this value is the actual concentration associated with cells: 6.95×10^{-4} M. Since cell numbers decreased significantly, multiplying by the fixed biomass concentration creates an artificially high value. (Also note: using bacterial data only, no archaeal data available; significant precipitation was observed in these samples, such that An associated with cells is overestimated)
- U(IV/VI): [(2.22×10^{-6} M associated with cells)/(2.30×10^{11} cells/L)]*10^{12} cells/L = 9.65×10^{-6} M
- Np(IV/V): [(2.74×10^{-8} M associated with cells)/(1.80×10^{11} cells/L)]*10^{12} cells/L = 1.52×10^{-7} M

Basis, Justification, and Calculations for An(III) Recommendations

A series of experiments has focused on the An(III) analog, neodymium, and its interaction with several WIPP microbial isolates in simple sodium chloride solutions and in WIPP brines (Swanson, 2022; Swanson et al., 2023; Swanson, 2024). All tested organisms had an influence on the concentrations of Nd in simplified NaCl and ERDA (i.e., Nd was removed from solution), but the loss of Nd from ERDA was slower. In contrast, there was little biological influence on Nd in GWB (i.e., Nd remained in solution), due to apparent competition between Nd and magnesium for cell surface sites.

There are more mechanisms involved in the loss of Nd from solution than simple surface complexation. Biosorption likely accounts for the Nd loss measured at the earliest time points of the experiments. However, the continued loss of Nd from solution in high-NaCl solutions over time is more likely to be due to precipitation or internal uptake. Regardless of whether internal uptake occurred, all cells settled out of suspension over time and are therefore not considered mobile, according to the parameter definitions. These additional loss mechanisms will lead to conservative overestimations of both PROPMIC and CAPMIC values.

PROPMIC and CAPMIC values were calculated using all data from the above experiments. Values were significantly higher in all experiments conducted in simple NaCl solution than in WIPP brines providing evidence that the background matrix is the dominant cause of the observed bioassociation trends (Figure 5).

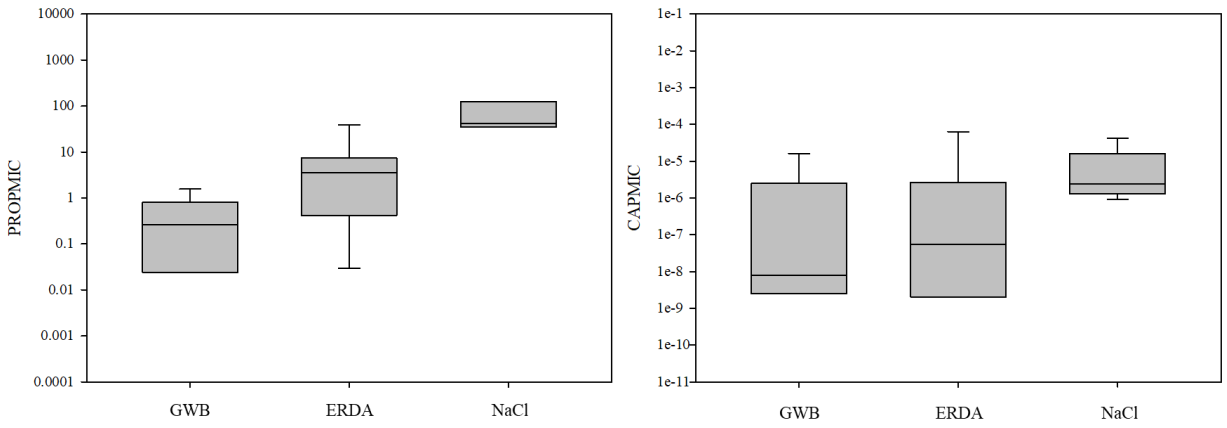

Figure 5. Box and whisker plots summarizing PROPMIC (left) and CAPMIC (right) data sets at the final time point of each experiment and across the three tested background matrices (from Swanson, 2024, Figures 14 and 15). The line transecting each box is the median, the upper bound of the box is the upper quartile value.

The new parameter values are taken from the experiments conducted in WIPP brines. Data from the final time point of all experiments were grouped, and the value delineating the upper quartile was chosen as the parameter value (i.e., 75% of all values are below this, Figure 5). This upper quartile was suggested by the EPA to be an acceptable value that bounds the majority of the data (EPA, 2022). However, the CAPMIC value calculations included cases where the biomass

concentration decreased by 2-3 orders of magnitude, thereby increasing the value (see Th case above). A decrease in biomass should, by definition, imply a decrease in microbe-bound actinide concentration, unless one assumes that uncounted dead cells also bind the actinide. If this assumption is made, then CAPMIC values actually decrease. The parameter values provided here are based on final biomass concentrations for tests in which cell numbers did not decrease significantly and on initial biomass concentrations for tests in which cell numbers did. An overall summary table is provided in Table 9.

Table 8. CAPMIC and PROPMIC values recommended for CRA-2026.

Parameter values for CAPMIC and PROPMIC recommended for CRA-2026		
Actinide (Oxidation State)	CAPMIC, M	PROPMIC
Th(IV)	6.95×10^{-4}	3.10×10^{0}
U(IV)	9.65×10^{-6}	2.10×10^{-3}
U(VI)		
Np(IV)	1.52×10^{-7}	1.20×10^{1}
Np(V)		
Pu(III)	4.97×10^{-7}	2.92×10^{0}
Pu(IV)	4.07×10^{-9}	3.00×10^{-1}
Am(III)	4.97×10^{-7}	2.92×10^{0}

Additional Comments

DOE has stated previously that biosorption results can vary depending upon many factors, including the organism and test matrix. The literature survey conducted by the EPA has also shown that biosorption data can be highly variable (EPA, 2022). Because of this variability, the DOE has emphasized that data should be generated using WIPP-relevant organisms under WIPP-relevant conditions. This approach may have narrowed the extent of the variability, but it is still present. Even so, the new data show some trends:

- The extent of biological influence on Nd in solution across the three tested matrices is: NaCl > ERDA >> GWB (i.e., more Nd is removed from simple NaCl than WIPP brines)
- Behavior is more similar between NaCl-based matrices (e.g., ERDA and simplified NaCl) than between ERDA and GWB
- There is a competitive effect of magnesium on the extent of biological influence
- The release of ligands, such as dipicolinate, from test organisms negates the colloid effect
- For PROPMIC:

    - Values can increase with time until they can no longer be defined (consequence of the method used to calculate PROPMIC)
    - Values are lower when the tested biomass concentration is lower
    - Values are lower in WIPP brines than in simplified NaCl solutions
- For CAPMIC:
    - Values do not vary significantly with time as PROPMIC values do
    - Values are higher when the tested biomass is lower
    - Values are lower in WIPP brines than in simplified NaCl solutions

The DOE can continue to conduct experiments on other oxidation states. This may result in further changes to parameter values for future CRAs. Finally, it should be noted that many conservatisms are already built into the PA colloid model.

- Each actinide is considered individually, such that each could theoretically associate to maximum capacity with each organism. This is impossible in reality, as there are a finite number of surface binding sites, and only one actinide can bind to a site at a time.
- Although PA refers to the mobile microbe population, current experiments are carried out using all microbes in suspension, not just those that might be considered mobile (i.e., suspended only).
- Results from current (and former) studies do not differentiate between actinide that has precipitated and that which is associated. This results in an overestimation of association. However, since this distinction is not made, the overestimation is accepted.
- Values are derived from experiments using uncomplexed actinides.

Table 9. Summary of historical values for PROPMIC and CAPMIC, suggested values, and new recommended values for CRA-2026.

Actinide (Oxidation State)	CCA through CRA-2009[1]		CRA-2014[1,2]		CRA-2019[1,3]		EPA Suggested Values[1,4]		Recommended values for CRA-2026	
	PROPMIC	CAPMIC, M	PROPMIC	CAPMIC, M	PROPMIC	CAPMIC, M	PROPMIC	CAPMIC, M	PROPMIC	CAPMIC, M
Th(IV)	3.1	1.9×10^{-3}	1.76	2.6×10^{-6}	0.21	3.8×10^{-8}	3.1	2.12×10^{-2}	3.1	6.95×10^{-4}
U(IV)	2.1×10^{-3}	2.1×10^{-3}	1.76	2.6×10^{-6}	0.21	3.8×10^{-8}	2.1×10^{-3}	8.14	2.1×10^{-3}	9.65×10^{-6}
U(VI)										
Np(IV)	12	2.7×10^{-3}	1.76	2.6×10^{-6}	0.21	3.8×10^{-8}	12	1.01×10^{-3}	12	1.52×10^{-7}
Np(V)										
Pu(III)	0.3	6.5×10^{-5}	1.76	2.6×10^{-6}	0.21	3.8×10^{-8}	2.18	2.18×10^{-5}	2.92	4.97×10^{-7}
Pu(IV)									0.3	4.07×10^{-9}
Am(III)	3.6	1	0.32	3.1×10^{-8}	0.03	2.3×10^{-9}	3.6	6.28×10^{-6}	2.92	4.97×10^{-7}

[1]element-specific
[2]bacterial values
[3]archaeal values originally presented in Reed, 2013; LCO-ACP-18
[4]EPA-HQ-OAR-2019-0534

5.0 References

Altmaier M, Neck V, Fanghänel T. 2004. Solubility and Colloid Formation of Th(IV) in Concentrated NaCl and $MgCl_2$ Solutions. *Radiochimica Acta* 92: 537-543.

Asami K, Kikucki M. 2003. In-Depth Distribution of Rusts on a Plain Carbon Steel and Weathering Steels Exposed to Coastal-Industrial Atmosphere for 17 Years. *Corrosion Science* 45: 2671-2688.

Beam J. 2022. Actinide (III/IV)-Silica Colloids in the WIPP. Report LCO-ACP-27. Los Alamos National Laboratory; Carlsbad, NM.

Beam J. 2023. Plutonium Oxidation State Distribution under WIPP-Relevant Conditions. Report LCO-ACP-31, Rev. 1.

Borkowski M, Lucchini J-F, Richmann MK, Reed DT. 2010. Actinide (III) Solubility in WIPP Brine: Data Summary and Recommendations. Report LCO-ACP-08. Los Alamos National Laboratory; Carlsbad, NM.

Borkowski M. 2012. Numerical Values for Graphs Presented in Report LCO-ACP-08, Entitled, Solubility of An(IV) in WPP Brine: Thorium analog Studies in WIPP Simulated Brine, and for Graphs Published in Borkowski, M et al., *Radiochimica Acta* 98: 577-582 (2010). Report ACP-01. Los Alamos National Laboratory; Carlsbad, NM.

Büppelmann K, Magirius S, Lierse C, Kim JI. 1986. Radiolytic Oxidation of Americium(III) to Americium(V) and Plutonium(IV) to Plutonium(VI) in Saline Solution. *Journal of the Less-Common Metals* 122: 329-336.

Büppelmann K, Kim JI, Lierse C. 1988. The Redox Behavior of Plutonium in Saline Solutions under Radiolysis Effects. Radiochimica Acta 44/45: 65-70.

Cook DC. 2005. Spectroscopic Identification of Protective and Non-Protective Corrosion Coatings on Steel Structures in Marine Environments. *Corrosion Science* 47: 2550-2570.

Dumas T, Fellhauer D, Schild D, Gaona X, Altmaier M, Scheinost AC. 2019. Plutonium Retention Mechanisms by Magnetite under Anoxic Conditions: Entrapment Versus Sorption. *ACS Earth and Space Chemistry* 3: 2197–2206.

Duro L, Domènech C, Grivé M, Roman-Ross G, Bruno J, Källström K. 2014. Assessment of the Evolution of the Redox Conditions in a Low and Intermediate Level Nuclear Waste Repository (SFR1, Sweden). *Applied Geochemistry* 49: 192-205.

Favela Morales D, Lucchini J-F. 2024. Radiolytic Degradation of Organics—Progress Report. Report LCO-ACP-39. Los Alamos National Laboratory; Carlsbad, NM.

Francis AJ, Gillow JB, Dodge CJ, Dunn M, Mantione K, Strietelmeier BA, Pansoy-Hjelvik ME, Papenguth HW. 1998. Role of Bacteria as Biocolloids in the Transport of Actinides from a Deep Underground Radioactive Waste Repository. *Radiochimica* Acta 82: 347-354.

Garnov AY, Yusov AB, Shilov VP, Krot NN. 1998. Reactions of Hypobromite with Neptunium (IV) and Plutonium (IV) in Alkali Solution. *Radiochemistry* 40: 17.

Hara S, Kamimura T, Miyuki H, Yamashita M. 2007. Taxonomy for Protective Ability of Rust Layers Using its Composition Formed on Weathering Steel Bridge. *Corrosion Science* 49: 1131-1142.

Kaplan U. 2024a. Plutonium Oxidation State Distribution in the Presence of WIPP-Relevant Organics and Iron Corrosion Products. Report LCO-ACP-38. Los Alamos National Laboratory; Carlsbad, NM.

Kaplan U. 2024b. Pu Oxidation State Distribution. Presentation for DOE-CBFO, Sept. 26, 2024. LA-UR-24-30637. Los Alamos National Laboratory; Carlsbad, NM.

Kim JI, Lierse C, Büppelmann K, Magirius S. 1987. Radiolytically Induced Oxidation Reactions of Actinide Ions in Concentrated Salt Solutions. *Materials Research Society Symposium Proceedings* 84: 603–612.

King F. 2008. Corrosion of Carbon Steel under Anaerobic Conditions in a Repository for SF and HLW in Opalinus Clay. NAGRA Technical Report 08-12 (National Cooperative for the Disposal of Radioactive Waste). Wettingen, Switzerland.

King S. 2025. S King, Letter to Jonathan Icenhower: Sandia's needs for WIPP parameter recommendations for Compliance Recertification Application 2026 Performance Assessment, January 24, 2025.

Kirsch R, Fellhauer D, Altmaier M, Neck V, Rossberg A, Fanghänel T, Charlet L, Scheinost AC. 2011. Oxidation State and Local Structure of Plutonium Reacted with Magnetite, Mackinawite, and Chukanovite. *Environmental Science & Technology* 45: 7267–7274.

Królikowska A, Komorowski L, Kunce I, Wojda D, Zacharuk K, Paszek U, Wierzbicki T, Bilewska K. 2021. Corrosion Assessment of a Weathering Steel Bridge Structure after 30 Years of Service. *Materials* 14: 3788.

Kutahyali Aslani C. 2024. Effects of Borate and Organics on U(VI) Solubility in WIPP Brine. Report LCO-ACP-33, Rev 1. Los Alamos National Laboratory; Carlsbad, NM.

Lucchini J-F, Khaing H, Borkowski M, Richmann MK, Reed DT. 2010. Actinide (VI) Solubility in Carbonate-Free WIPP Brine: Data Summary and Recommendations. LCO-ACP-10. Los Alamos National Laboratory; Carlsbad, NM.

Lucchini J-F, Richmann MK, Borkowski M. 2013. Uranium(VI) Solubility in WIPP Brine. Report LCO-ACP-14. Los Alamos National Laboratory; Carlsbad, NM.

Lucchini J-F, Swanson J. 2023. LANL ACRSP Parameter Recommendations for CRA-2024 Performance Assessment. Report LCO-ACP-34. Los Alamos National Laboratory; Carlsbad, NM.

Papenguth HW. 1996. HW Papenguth to Christine Stockman: Parameter Record Package for Colloidal Actinide Source Term Parameters: Attachment A: Rationale for Definition of Parameter Values for Microbes. Attachment A: WPO#35856. Sandia National Laboratories; Albuquerque, NM.

Pashalidis I, Lierse C, Sullivan JC, Kim JI. 1993. The Chemistry of Pu in Concentrated Aqueous NaCl Solution: Effects of Alpha Self-Radiolysis and the Interaction between Hypochlorite and Dioxoplutonium (VI). *Radiochimica Acta* 60: 99–101.

Peake T. 2020. Fourth Set of EPA Completeness Comments and Questions for Compliance Recertification application 2019 (CRA-2019). US Environmental Protection Agency, Center for Waste Management and Regulation, Washington, DC. Letter to M Brown, US Department of Energy, Carlsbad Field Office, Carlsbad, NM. July 17, 2020.

Reed DT, Swanson J, Lucchini J-F, Richmann MK. 2013. Intrinsic, Mineral and Microbial Colloid Enhancement Parameters for the WIPP Actinide Source Term. LCO-ACP-18. Los Alamos National Laboratory; Carlsbad, NM.

Reed DT, Swanson J, Stanley F. 2019. LANL/ACRSP Parameter Recommendations for the CRA-2019 Deferred Performance Assessment. Report LCO-ACP-24, Rev 1. Los Alamos National Laboratory; Carlsbad, NM.

Saheb M, Neff D, Demory J, Foy E, Dillman P. 2010. Characterization of Corrosion Layers Formed on Ferrous Archaeological Artefacts Buried in Anoxic Media. *Corrosion Engineering and Science Technology* 45: 381-387.

Schramke JA, Santillan EFU, Peake RT. 2020. Plutonium Oxidation States in the Waste Isolation Pilot Plant Repository. *Applied Geochemistry* 116: 104561.

Swanson J. 2022. Biologically Influenced Transport of the +3 Actinide Oxidation State from the WIPP Environment, Using Neodymium as an Analog. LCO-ACP-32, Rev. 0. Los Alamos National Laboratory; Carlsbad, NM.

Swanson J, Navarrette A, Knox J, Kim H, Stanley F. 2023. Microbial Influence on the Mobility of +3 Actinides from a Salt-Based Nuclear Waste Repository. *Microorganisms* 2023: 11061370.

Swanson J. 2024. Biologically Influenced Transport of the +3 Actinide Oxidation State from the WIPP Environment, Using Neodymium as an Analog. Report LCO-ACP-32, Rev 1. Los Alamos National Laboratory; Carlsbad, NM.

Toste AP. 1992. Degradation of Chelating and Complexing Agents in an Irradiated, Simulated Mixed Waste. *Journal of Radioanalytical and Nuclear Chemistry, Articles* 161: 549-559.

Toste AP, Polach KJ, White TW. 1994. Degradation of Citric Acid in a Simulate, Mixed Nuclear Waste: Radiolytic versus Chemical Forces. *Waste Management* 14: 27-34.

US Department of Energy. 1996. Title 40 CFR Part 191 Compliance Certification Application for the Waste Isolation Pilot Plant (October). 21 vols. DOE/CAO-1996-2184. Carlsbad, NM; Carlsbad Field Office.

US Department of Energy. 2019. Title 40 CFR Part 191 Compliance Recertification Application for the Waste Isolation Pilot Plant (March). Carlsbad, NM; Carlsbad Field Office.

US Department of Energy. 2019 Compliance Recertification Application, Appendix PA-2019.

US Department of Energy. 2019 Compliance Recertification Application, Appendix SOTERM-2019.

US Environmental Protection Agency. 2005. Letter from E Cotsworth to I Triay (US DOE-CBFO), March, 2005. Conducting the Performance Assessment Baseline Change Verification Test.

US Environmental Protection Agency. 2022. Technical Support Document for Section 194.24: Evaluation of the Compliance Recertification Application (CRA-2019) Actinide Source Term, Gas Generation, Backfill Efficacy, Water Balance, and Culebra Dolomite Distribution Coefficient Values. EPA-HQ-OAR-2019-0534.

US Environmental Protection Agency. 2023. Memo from T Peake to M Bollinger (US DOE-CBFO). Schedule for Future Compliance Recertification Application Submittals.

Van Soest GD. 2022. Performance Assessment Inventory Report—2022. Report INV-PA-22. Los Alamos National Laboratory; Carlsbad, NM.